

# Impact of UV Light Exposure During Printing on Thermomechanical Properties of 3D-Printed Polyurethane-Based Orthodontic Aligners

---

Šimunović, Luka; Marić, Antun Jakob; Bačić, Ivana; Haramina, Tatjana; Meštrović, Senka

Source / Izvornik: **Applied Sciences**, 2024, 14

Journal article, Published version

Rad u časopisu, Objavljena verzija rada (izdavačev PDF)

<https://doi.org/10.3390/app14209580>

Permanent link / Trajna poveznica: <https://um.nsk.hr/um:nbn:hr:127:782943>

Rights / Prava: [Attribution 4.0 International](#) / [Imenovanje 4.0 međunarodna](#)

Download date / Datum preuzimanja: **2025-03-14**



Repository / Repozitorij:

[University of Zagreb School of Dental Medicine  
Repository](#)



## Article

# Impact of UV Light Exposure During Printing on Thermomechanical Properties of 3D-Printed Polyurethane-Based Orthodontic Aligners

Luka Šimunović <sup>1</sup> , Antun Jakob Marić <sup>2</sup> , Ivana Bačić <sup>3</sup> , Tatjana Haramina <sup>4</sup> and Senka Meštrović <sup>1,\*</sup> 

<sup>1</sup> Department of Orthodontics, School of Dental Medicine, University of Zagreb, 10000 Zagreb, Croatia; lsimunovic@sfzg.unizg.hr

<sup>2</sup> Faculty of Mechanical Engineering and Naval Architecture, University of Zagreb, 10000 Zagreb, Croatia; antun@3dtech.hr

<sup>3</sup> Forensic Science Centre “Ivan Vučetić”, Ministry of the Interior, 10000 Zagreb, Croatia; ivana.bacic@mup.hr

<sup>4</sup> Department of Materials, Faculty of Mechanical Engineering and Naval Architecture, University of Zagreb, 10000 Zagreb, Croatia; tatjana.haramina@fsb.unizg.hr

\* Correspondence: mestrovic@sfzg.unizg.hr

**Abstract:** Aim: Polyurethane-based aligners, created through photoinitiated free-radical polymerization, have been the subject of numerous studies focusing solely on their mechanical properties. In contrast, we investigate their thermomechanical properties, which are crucial for their efficacy. This paper aims to investigate the effects of different UV light exposure durations on the complex modulus of elasticity, tan delta, glass transition temperature, and the degree of conversion (DC). Methods: Aligners were printed using Tera Harz TC-85 and NextDent Ortho Flex resin with specific exposure times (2, 2.4, 3, 4, and 4.5 s for Tera Harz; 5, 6, 7, and 8 s for NextDent) and processed per manufacturer guidelines. The degree of conversion was analyzed using Attenuated Total Reflectance Fourier Transform Infrared (ATR-FTIR) spectroscopy, while Dynamic Mechanical Analysis (DMA) characterized the mechanical properties (complex modulus and tan delta) and the glass transition. Results: Tera Harz TC-85 showed a higher degree of conversion (90.29–94.54%), suggesting fewer residual monomers, which is potentially healthier for patients. However, its lower glass transition temperature (35.60–38.74 °C) might cause it to become rubbery in the mouth. NextDent Ortho Flex, with a higher storage modulus (641.85–794.55 MPa) and  $T_g$  (49.36–50.98 °C), offers greater rigidity and stability at higher temperatures (greater than temperature in the oral cavity), ideal for orthodontic forces, though its lower degree of conversion raises health concerns. Conclusions: Tera Harz TC 85 generally achieves higher DC and more stable polymerization across different UV exposure times than NextDent Ortho Flex. Optimal polymerization times significantly impact both the mechanical and thermal properties of these dental resins, with NextDent showing optimal properties at 7 s and Tera Harz benefiting from both very short and extended exposure times.



**Citation:** Šimunović, L.; Marić, A.J.; Bačić, I.; Haramina, T.; Meštrović, S. Impact of UV Light Exposure During Printing on Thermomechanical Properties of 3D-Printed Polyurethane-Based Orthodontic Aligners. *Appl. Sci.* **2024**, *14*, 9580. <https://doi.org/10.3390/app14209580>

Academic Editor: Gaetano Paolone

Received: 16 September 2024

Revised: 13 October 2024

Accepted: 18 October 2024

Published: 21 October 2024

**Keywords:** aligners; 3D printing; Fourier Transform Infrared spectroscopy; dynamic mechanical analysis



**Copyright:** © 2024 by the authors. Licensee MDPI, Basel, Switzerland. This article is an open access article distributed under the terms and conditions of the Creative Commons Attribution (CC BY) license (<https://creativecommons.org/licenses/by/4.0/>).

## 1. Introduction

Aligners, particularly those made from polyurethane, are popular in orthodontics for their aesthetic appeal and comfort compared to traditional fixed orthodontic treatment, which includes brackets and wires [1]. These clear, removable devices gradually move teeth into their desired positions using a series of custom-made aligners, each slightly different from the previous one [2]. The effectiveness of aligners depends significantly on their material properties, which must balance rigidity to exert adequate force and flexibility for patient comfort [3]. The production of clear aligners generally falls into two categories: thermoforming and 3D printing. Thermoforming involves heating a polymer sheet to make it flexible, then shaping it over a dental model to create the aligner. This technique

utilizes thermoplastic resin polymers, including materials like poly(vinyl chloride) (PVC), poly(ethylene terephthalate) (PET), poly(ethylene terephthalate glycol) (PETG), and thermoplastic polyurethane (TPU). In contrast, 3D printing, also known as additive manufacturing, constructs the aligner by adding material layer by layer from a digital model. These aligners are typically made from polyurethane-based materials, selected for their combination of clarity, durability, and flexibility—key factors needed for applying consistent force to reposition teeth. Polyurethane, in particular, stands out for its excellent mechanical properties and the comfort it provides to patients [3–5]. Three-dimensional printing has revolutionized the production of aligners, allowing for precise customization and rapid production [6]. Photocurable resins are categorized into two primary types based on their polymerization mechanisms: photoinitiated free-radical polymerizations and photoinitiated cationic polymerizations [7]. Free-radical polymerizations include the polymerization of acrylates, while cationic polymerizations encompass the polymerization of epoxides, lactones, and vinyl ethers, which are not affected by radicals. A significant advantage of cationic polymerizations is their resistance to atmospheric oxygen, unlike free-radical polymerizations, which suffer from oxygen inhibition where radicals are lost to oxygen [7]. Polyurethane-based aligners, made by photoinitiated free-radical polymerization, have been the subject of numerous studies focusing on their mechanical and thermal properties, which are crucial for their efficacy in orthodontic applications [8]. Previous *in vitro* research has shown that manufacturing and post-processing conditions, such as UV light exposure during manufacturing, rinsing, and polymerization in a different environment, as well as the use of different 3D printers, affect the mechanical properties of 3D-printed aligners [9–15]. These investigations aim to optimize the aligners' performance by understanding the impact of factors like UV curing during post-processing on their structural integrity and longevity. However, the mechanical properties of the aligner material, influenced by factors such as UV curing during 3D printing, play a critical role in their overall performance and durability [16]. It is important to note that while UV light exposure in the post-processing phase has been studied, the effect of UV exposure on the layers during the 3D printing process has not yet been investigated thoroughly. The mechanical properties of polyurethane-based aligners are critical for their performance and longevity in orthodontic treatments, as they determine the aligners' ability to maintain shape, resist deformation, and perform under stress [17,18]. Several 3D printing parameters, including the type and intensity of UV light used during curing, the duration of UV exposure, the printing temperature, and post-processing conditions, significantly impact the mechanical and thermal properties of the aligners [19–21]. The modulus of elasticity, which is the measure of the stiffness of the aligner material, is crucial for the aligners to apply the necessary orthodontic forces while maintaining flexibility for comfort [8]. Generally, UV exposure can lead to photodegradation and photo-oxidation, impacting the modulus of elasticity, with initial exposure increasing the modulus. Still, prolonged exposure potentially reduces it due to material degradation [22,23]. Tan delta, a measure of the damping properties and viscoelastic behavior of the material, is also influenced by UV exposure [24]. This parameter is critical for understanding how the aligners dissipate energy as heat. UV exposure increases tan delta, indicating more energy dissipation, but extended exposure may decrease it due to the material becoming more brittle [25,26]. The transition temperature, particularly the glass transition temperature ( $T_g$ ), signifies the temperature at which the polymer transitions from a hard, glassy state to a soft, rubbery state [27,28]. A suitable  $T_g$  is essential for aligners to perform effectively across various temperatures [8]. UV light exposure, especially its energy density and power density, can lower the  $T_g$  by increasing the degree of cross-linking and reducing chain mobility [29–31]. Understanding the effects of UV exposure on  $T_g$  helps in designing aligners that maintain their properties under different environmental conditions in the oral cavity. The degree of conversion (DC) reflects the extent to which monomers have transformed into polymers during the curing process. A higher degree of conversion typically results in better mechanical properties and chemical resistance of the aligners [11]. UV exposure affects the DC, with higher intensity and longer exposure times generally

increasing the DC. However, excessive exposure can lead to over-curing or degradation, which may negatively impact the DC, resulting in compromised mechanical properties [29]. Proper control of UV exposure is necessary to achieve an optimal balance, ensuring the aligners have the desired mechanical properties without compromising their structural integrity. This paper aims to investigate the effects of different UV light exposure durations on the modulus of elasticity, glass transition temperature, tan delta, and the degree of the conversion of polyurethane-based aligners. By understanding these relationships, we can optimize 3D printing parameters to enhance the performance and durability of orthodontic aligners, ensuring they meet the required standards for effective orthodontic treatment.

## 2. Materials and Methods

### 2.1. Sample Preparation

Aligner samples 1 mm × 3 mm × 12 mm (thickness × width × length) were printed using Tera Harz TC-85 resin (Graphy, Seoul, Republic of Korea) and NextDent Ortho Flex (Vertex-Dental B.V., Soesterberg, The Netherlands). Exposure times of 5 s, 6 s, 7 s, and 8 s for NextDent and 2 s, 2.4 s, 3 s, 4 s, and 4.5 s for Tera Harz were used. These resins, intended for use in the digital light processing method, were printed in consecutive layers of a nominal thickness of 100 µm. The printing was carried out on a SprintRay Pro 95 (SprintRay, Los Angeles, CA, USA). Post-processing and post-curing were carried out as proposed by the manufacturer, which includes centrifuging 2× for 5 min and post-curing for 20 min in the Tera Harz Cure THC2 (Graphy, Seoul, Republic of Korea). Samples with an exposure time of 7 s were considered the control group for NextDent Ortho Flex, while for the Tera Harz TC-85 resin control group was 4 s, as proposed by the pilot study. For each group, 10 samples were prepared (in total, 90 samples).

### 2.2. Material Identification and Degree of Conversion

Fourier Transform Infrared Spectroscopy (FTIR) coupled with the Attenuated Total Reflectance (ATR) technique was used to identify the resins in both liquid and polymerized forms, and changes in their spectra were used to determine the polymerization effect or the degree of conversion. Aligner samples were measured at 10 positions of the outer layers and 5 in the inner layer and then directly analyzed on a Bruker ALPHA ATR-FTIR spectrometer (Bruker, Ettlingen, Germany) with a diamond as the single reflection element under standard analysis conditions (wavenumber range 4000–400 cm<sup>-1</sup>, resolution 4 cm<sup>-1</sup>, 10 scans per spectrum). The Savitzky–Golay algorithm was used to process the spectra and improve the signal-to-noise ratio as needed. The degree of conversion (DC) is calculated from the following equation:

$$DC(\%) = (A_{LR} - A_P) / A_{LR} \times 100$$

where  $A_{LR}$  and  $A_P$  are the absorbance intensities in liquid resins and after polymerization, respectively. Absorbance intensities are automatically generated from derivative spectra by the Bruker OPUS 8.8 software.

### 2.3. Characterization of Material Structure and Glass Transition

Dynamic Mechanical Analysis (DMA) was used to characterize the structure of 3D-printed polyurethane-based aligners. The tests were conducted on a TTDMA (Triton Technology/Mettler Toledo, Columbus, OH, USA). DMA is the most sensitive known method for tracking changes in material structure [32]. The mentioned TTDMA device can conduct measurements with a frequency from 0.001 to approximately 500 Hz, over a temperature range of −190 °C to 600 °C. For project purposes, testing was conducted at a frequency of 1 Hz to facilitate comparison with literature-published data, and the temperature interval was determined according to the needed material characteristics, 20 to 100 °C. This method measures the damping of mechanical vibrations due to a phase shift  $\delta$  between stress and strain (loss factor,  $\tan \delta$ ) in the material over a specified temperature range during constant heating and/or cooling rate, and the corresponding complex

modulus of elasticity  $E^* = E' + iE''$ . The complex modulus is time or frequency dependent and consists of a real component  $E'$ , which is the storage modulus, and the imaginary component  $E''$ , which is the loss modulus. The former represents the energy stored in the material during the dynamic loading, and the latter represents the dissipated energy. The loss factor  $\tan \delta$  is equal to the ratio of  $E''/E'$ . In the case of pure elastic behavior, the storage modulus equals the elastic modulus and the  $\delta$  is equal to zero. Although the  $E'$  is time dependent, it is comparable to the elastic modulus measured at the tensile test machine and is a useful parameter for the characterization of the materials. During dynamic loading, deformation amplitudes are very small to assure anelastic behavior, i.e., there is not any plastic deformation of materials, and the cycle can be repeated several times if justified [33]. Any change in structure is reflected in the mechanical spectrum. At low temperatures, changes in the part of the structure with high eigenfrequencies, such as rotations of side groups, are monitored, while at higher temperatures, changes in whole chains or segments of polymer chains are tracked, allowing a precise monitoring of the glass transition. Testing was conducted on printed specimens in the form of a cuboid, with a maximum width of 3 mm, a thickness of 1 mm, and a length of 12 mm. The distance between the clamps was 7.5 mm. Due to the complexity of measurements and the detailed analysis of results, the justification for repeating cycles was determined based on the results of the first cycle for individual samples. Although the DMA method is sensitive to changes in the material, it requires measurements on samples of defined dimensions and sufficient rigidity, thus it is limited to temperatures below the melting point.

#### 2.4. Sample Size

To ensure robust statistical analysis through two-way ANOVA, the required sample size to detect a small effect size ( $f = 0.25$ ) with an  $\alpha$  error probability of 0.05 and a power of 80% was calculated. Calculations showed a required sample size of 10 per group to achieve the desired power.

#### 2.5. Statistical Analysis

The statistical analysis aimed to investigate the storage modulus ( $E'$ ), glass transition temperature ( $T_g$ ), and the degree of conversion (DC) across different brands and UV exposure groups. QQ plots, the Shapiro–Wilk test, and calculations of skewness and kurtosis were used to check the normality of the data. The Mann–Whitney U test was utilized to compare the  $E'$ ,  $T_g$ , and DC between different brands due to its robustness against non-normal data distributions. For comparisons among the various UV exposure groups, the Kruskal–Wallis test followed by the post hoc Dunn test was employed. To assess the relationships among  $E'$ ,  $T_g$ , and DC, the Spearman rank correlation was used, due to non-linear relationships. All statistical analyses were performed using the IBM SPSS Statistics software, version 29.0.1.0 (IBM, New York, NY, USA), with a  $p$ -value of less than 0.05 considered statistically significant for all tests.

### 3. Results

#### 3.1. Degree of Conversion (DC)

FTIR spectra of liquid (resin) and polymerized NextDent Ortho Flex and Graphy material are shown in Figure 1, while the spectra of Tera Harz TC-85 resin are described in detail in previous studies [11,15]. The spectrum of the liquid sample of NextDent Ortho Flex material indicates a complex mixture of initial monomers, where the vibrational bands of methacrylate can be distinguished, which are more abundant compared to the spectrum of the liquid Tera Harz TC-85 material (Table 1). The presence of the carbonyl group is indicated by a stretching vibration at  $1715\text{ cm}^{-1}$ , followed by a medium absorption with a maximum at  $1650\text{ cm}^{-1}$ , which is contributed by the stretching vibration of the aliphatic C=C group visible as a slightly pronounced shoulder at  $1638\text{ cm}^{-1}$ . The presence of an aliphatic C=C group is also proven by an additional band at  $1617\text{ cm}^{-1}$  as well as the sharp band of twisting vibrations at  $810\text{ cm}^{-1}$ . Symmetric and antisymmetric deformations

and the stretching of methyl and methylene groups are visible as medium bands in the range  $\sim 1500\text{--}1350\text{ cm}^{-1}$  and  $\sim 3000\text{--}2820\text{ cm}^{-1}$ , respectively. Below  $1350\text{ cm}^{-1}$ , many strong C-C-O and C-O-C stretching vibrations can be seen. Absorption bands at  $980\text{ cm}^{-1}$  and  $847\text{ cm}^{-1}$  have been attributed to the C-H rocking and skeletal C-C stretching mode, while maxima at  $754\text{ cm}^{-1}$  (aromatic C-H wagging) and  $693\text{ cm}^{-1}$  (the bending of the aromatic ring) imply the presence of aromatic functional groups that are significantly smaller in the Tera Harz TC-85 material [34,35].

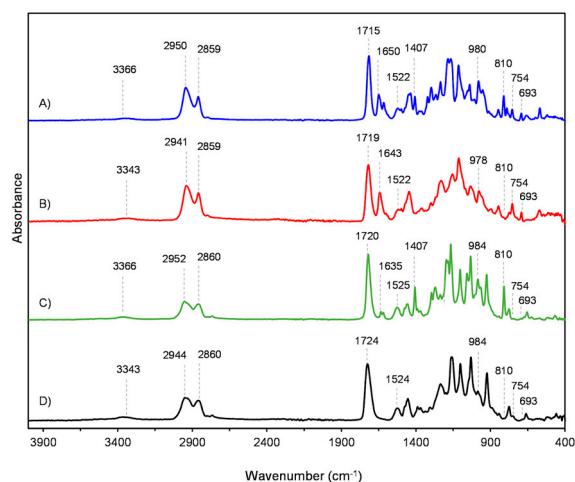


**Figure 1.** FTIR spectra (A) NextDent Orto Flex resin, (B) NextDent Orto Flex printed, (C) Tera Harz TC85 resin, and (D) Tera Harz TC85 printed.

**Table 1.** FTIR peak identification for the NextDent Orto Flex resin.

| Wavenumber ( $\text{cm}^{-1}$ ) | Vibration   |
|---------------------------------|---|
| 3343                            | $\nu$ N-H   |
| 2941                            | $\nu_{\text{as}}$ C-H ( $\text{CH}_2$ , $\text{CH}_3$ ) |
| 2859                            | $\nu_{\text{s}}$ C-H ( $\text{CH}_2$ , $\text{CH}_3$ )  |
| 1715                            | $\nu$ C=O (ester)                                       |
| 1650                            | $\nu$ C=O (amide)                                       |
| 1638                            | $\nu$ C=C   |
| 1617                            | $\nu$ C=C   |
| 1522                            | $\delta$ N-H  |
| 1407                            | $\delta$ $\text{CH}_2$                                  |
| $\sim 1350\text{--}1000$        | $\nu$ C-O-C   |
|                                 | $\nu$ C-C-O   |
| 980                             | $\delta_{\text{rc}}$ C-H                                |
| 847                             | $\nu$ C-C   |
| 810                             | $\delta_{\text{tw}}$ C=C                                |
| 754                             | $\delta_{\text{wg}}$ C-H (aromatic)                     |
| 693                             | $\delta$ aromatic ring                                  |

Abbreviations:  $\nu$  = stretching,  $\delta$  = bending, s = symmetric, as = asymmetric, rc = rocking, tw = twisting, and wg = wagging.

The spectra also contain absorption features associated with N-H stretching ( $3343\text{ cm}^{-1}$ ) and bending vibrations ( $1522\text{ cm}^{-1}$ ) as a characteristic of urethane compounds. The differences in the FTIR spectra of the initial mixture and the polymerized material are primarily visible through the loss or diminishing of the bands mainly related to the C=C bonds ( $1617$ ,  $810\text{ cm}^{-1}$ ) and C-H and C-O bonds ( $1407$ ,  $1322$ ,  $1297\text{ cm}^{-1}$ , etc.) in the monomers, which can be used, more or less successfully, to monitor the extent of polymerization. In this paper, according to the previous study, the degree of conversion for both resin materials was determined by a peak at  $810\text{ cm}^{-1}$ , originating from twisting vibrations of carbon-carbon methacrylate double bonds [11]. To enhance the resolution of the chosen band and

eliminate possible baseline shifts between samples, the Savitzky–Golay algorithm (second derivative with nine smoothing points) was applied. The DC is presented in Figure 2.

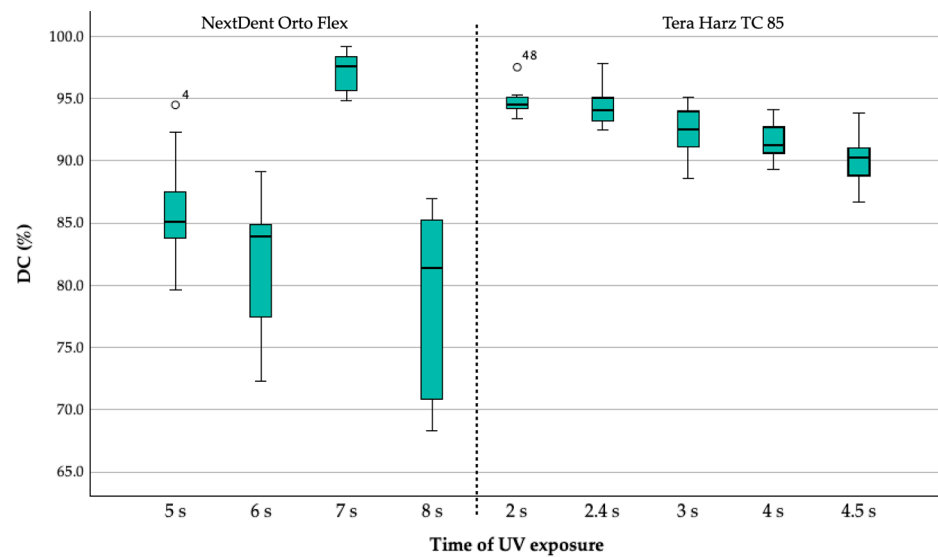


**Figure 2.** Degree of conversion (DC, %).

The DC was analyzed for two brands, NextDent Orto Flex and Tera Harz TC 85, under varying durations of UV exposure. For NextDent Orto Flex, the DC values were significantly lower at 5 s ( $p = 0.003$ ), 6 s ( $p < 0.001$ ), and 8 s ( $p < 0.001$ ) compared to the control at 7 s (Median = 97.55%). This indicates that the optimal polymerization time for NextDent Orto Flex is 7 s, with both shorter and longer exposures resulting in reduced DC. For Tera Harz TC 85, the DC values were significantly different at 2 s ( $p = 0.004$ ) compared to the control at 4 s (Median = 91.28%). The exposure times of 2.4 s, 3 s, and 4.5 s did not show significant differences from the control. This suggests that Tera Harz TC 85 maintains a relatively stable DC around the 4 s exposure time, with 2 s showing a higher DC. Overall, Tera Harz TC 85 exhibited higher DC rates than NextDent Orto Flex across the tested exposure durations, indicating better polymerization efficiency.

### 3.2. Storage Modulus ( $E'$ )

The test results indicated a statistically significant difference in the distribution of  $E'$  between the brands (Mann–Whitney  $U = 0.0$ , Wilcoxon  $W = 1275.0$ ,  $Z = -8.12$ ,  $p < 0.001$ ), which indicates that NextDent exhibits higher values across all times compared to Tera Harz. When considering the 7 s polymerization time as the control group of NextDent, the analysis shows that the  $E'$  at 5 s and 6 s polymerization times is significantly lower compared to the control. Specifically, the differences occur between the 5 s and control ( $p = 0.001$ ) and between the 6 s and control ( $p = 0.001$ ). In contrast, the difference between the 8 s and control polymerization times is not significant, indicating that the storage modulus for 8 s is comparable to that of the control. Thus, shorter polymerization times (5 s and 6 s) result in a significantly lower elastic modulus, while the longer polymerization time (8 s) does not differ significantly from the control. When comparing the storage modulus of different polymerization times to the 4 s control for Tera Harz TC-85, no significant difference is observed between the 3 s and 4 s times. The 2.4 s time shows no significant difference from the 4 s control after adjustment. However, significant differences are found between the 4 s control and both the 2 s and 4.5 s polymerization times, with these shorter and longer times having significantly higher storage modulus values compared to the 4 s control (Figure 3).

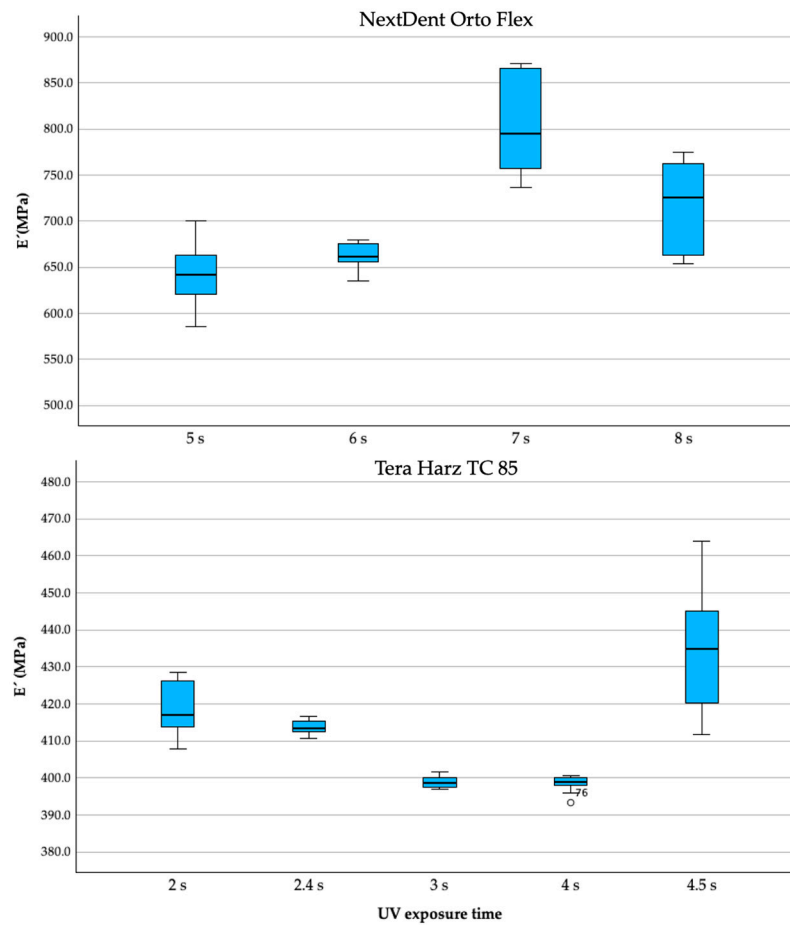


**Figure 3.** Storage modulus (MPa).

### 3.3. Glass Transition Temperature ( $T_g$ )

There is a statistically significant difference in the distribution of the  $T_g$  across the different resin brands, with NextDent being higher. The  $T_g$  values of NextDent for the 7 s and 8 s polymerization times are similar. Significant differences were observed between the 7 s and both the 6 s and 5 s times, with the  $T_g$  at 7 s being lower. On the other hand, the Tera Harz TC-85  $T_g$  values for the 2 s, 2.4 s, and 3 s polymerization times are similar to the 4 s control. However, the  $T_g$  for the 4.5 s time is significantly higher than the 4 s control (Figure 4).

Correlation analysis among three variables: storage modulus, glass transition temperature, and the degree of conversion presented that there is a strong and significant positive correlation between the  $E'$  and  $T_g$  (Spearman’s rho correlation coefficient 0.693,  $p < 0.001$ ), indicating these properties tend to increase together. There is a moderate and significant negative correlation between  $T_g$  and DC (rho  $-0.485$ ,  $p < 0.001$ ), suggesting that higher  $T_g$  is associated with lower DC. The correlation between  $E'$  and DC is weak and not significant (rho  $-0.187$ ,  $p = 0.077$ ) (Table 2).

**Table 2.** Correlation analysis (\*\* correlation is significant at the 0.01 level (2-tailed)).

|      |                         | $E'$  | $T_g$    | DC       |
|------|-------------------------|-------|----------|----------|
| $E'$ | Correlation coefficient | 1.000 | 0.693 ** | $-0.187$ |
|      | ( $p$ value)            | .     | $<0.001$ | 0.077    |



Table 2. Cont.

|    |                         | E'       | Tg        | DC        |
|----|-------------------------|----------|-----------|-----------|
| Tg | Correlation coefficient | 0.693 ** | 1.000     | −0.485 ** |
|    | (p value)               | <0.001   | .         | <0.001    |
| DC | Correlation coefficient | −0.187   | −0.485 ** | 1.000     |
|    | (p value)               | 0.077    | <0.001    | .         |

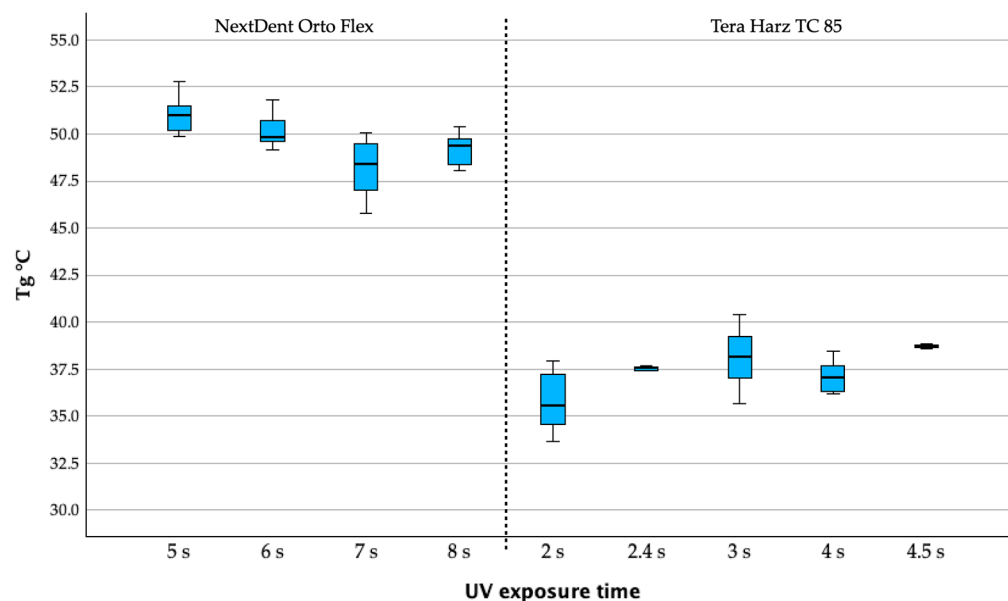


Figure 4. Glass transition temperature (°C).

#### 4. Discussion

Taking into consideration the above mentioned, our study reveals significant differences in the degree of conversion between two dental resin brands, NextDent Orto Flex and Tera Harz TC-85, under varying UV exposure durations while printing. For the NextDent Orto Flex, the optimal polymerization time was found to be 7 s, as both shorter (5 and 6 s) and longer (8 s) exposures resulted in significantly lower DC. This decline in DC at non-optimal exposure times can be attributed to insufficient cross-linking at shorter durations and the potential degradation of the photoinitiators or polymer matrix at longer durations. These results align with previous findings that excessive UV exposure can degrade photoinitiators and cause oxygen inhibition, leading to incomplete polymerization [36,37]. Conversely, Tera Harz TC 85 maintained relatively stable DC values around a 4 s exposure, with only the 2 s exposure showing a significant difference. This stability indicates that Tera Harz TC 85 has a more robust photoinitiation system that efficiently initiates polymerization even at shorter exposure times without detrimental overexposure effects. The higher overall DC rates for Tera Harz TC 85 compared to NextDent Orto Flex could be due to a more effective photoinitiator or a formulation that better resists the negative effects of UV overexposure, such as thermal degradation and oxygen inhibition [38,39]. However, numerous strategies have been suggested in the literature to mitigate oxygen inhibition in photopolymerizations [37,40,41]: (1) increasing the light dose or intensity, (2) raising the photoinitiator concentration, (3) employing co-initiators, (4) adding radical scavengers, (5) conducting the process in an inert environment, and (6) utilizing chemical mechanisms such as thiol-ene and thiol-acrylate-Michael systems, which are less sensitive to oxygen. The differences in the degree of conversion and their response to UV exposure duration highlight the importance of optimizing curing parameters for different materials to achieve

the best polymerization outcomes. These findings are consistent with the earlier studies that show that both the duration of UV exposure and the formulation of the photoinitiator system play crucial roles in determining the final mechanical and thermal properties of photopolymerized materials [42,43]. The storage modulus ( $E'$ ) is a critical parameter for evaluating the stiffness and rigidity of polymer-based dental resins, directly influencing their performance and durability in dental applications. NextDent generally exhibits higher  $E'$  values compared to Tera Harz, indicating that it forms a stiffer material. The presence of aromatic functional groups in NextDent, indicated by maxima at  $754\text{ cm}^{-1}$  and  $693\text{ cm}^{-1}$  (aromatic C-H wagging and the bending of the aromatic ring), indicates enhanced rigidity due to the planar structure and strong intermolecular interactions ( $\pi$ - $\pi$  interactions) of these groups [44]. In contrast, Tera Harz TC 85 has significantly fewer aromatic groups, which may contribute to its lower rigidity and, consequently, a lower storage modulus. Additionally, the higher intensity of absorption bands at  $980\text{ cm}^{-1}$  and  $847\text{ cm}^{-1}$  in Tera Harz TC 85, attributed to C-H rocking and skeletal C-C stretching modes, indicates a more flexible polymer chain structure, potentially reducing the storage modulus. Shorter polymerization times (5 and 6 s) of NextDent Orto Flex result in significantly lower  $E'$  values compared to the 7 s control, likely due to incomplete polymerization and cross-linking. This indicates that adequate polymerization time is crucial for achieving optimal stiffness. Increasing the polymerization time to 8 s does not significantly enhance  $E'$  beyond the 7 s control, indicating a threshold beyond which additional curing does not further improve stiffness. These findings are consistent with the previous research, which shows that increased polymerization times enhance the degree of cross-linking, thereby improving the mechanical properties of dental resins [45,46]. For Tera Harz TC 85, the storage modulus analysis indicates that the 4 s polymerization time serves as a reliable control. No significant differences in  $E'$  are observed between the 3 s and 4 s times or between the 2.4 s and 4 s times, indicating similar stiffness for these durations. However, significant differences are found between the 4 s control and both the 2 s and 4.5 s polymerization times, with these shorter and longer exposure times resulting in higher  $E'$  values. The higher  $E'$  at 2 s could be due to a rapid initial reaction, leading to an unexpectedly efficient cross-linking. The increased  $E'$  at 4.5 s indicates that extended polymerization enhances the cross-link density, resulting in a stiffer material. These results align with the literature, suggesting that both insufficient and extended polymerization can lead to increased material stiffness due to variations in the degree of cross-linking and polymer network formation [47–50]. Both NextDent Orto Flex and Tera Harz TC 85 show that the polymerization time critically affects the storage modulus. For NextDent, a polymerization time of around 7 s appears optimal, while for Tera Harz, both very short and extended times (2 s and 4.5 s) enhance stiffness. The glass transition temperature ( $T_g$ ) is a critical metric for evaluating the thermal properties of polymer-based dental resins, as it indicates the temperature at which a material shifts from a glassy, rigid state to a rubbery, flexible state. Understanding  $T_g$  helps in determining the material's performance and stability under different conditions [27,28]. In the context of NextDent and Tera Harz resins, the polymerization time significantly influences  $T_g$ , reflecting the extent of polymer cross-linking and the resulting thermal stability of the material. NextDent demonstrates a higher  $T_g$  compared to Tera Harz, indicating a more tightly bound polymer network and thus greater thermal stability. Aromatic groups can increase  $T_g$  due to restricted chain mobility and increased intermolecular forces [51], implying that the lower presence of aromatic groups in Tera Harz TC 85 compared to NextDent Orto suggests that Tera Harz TC 85 might have a lower  $T_g$ , leading to earlier softening upon heating. The study indicates that reducing the polymerization time to 5 or 6 s decreases  $T_g$  significantly, pointing to a less stable thermal structure. Conversely, extending the polymerization time to 8 s does not notably affect  $T_g$ , indicating an optimal polymerization time of around 7 s for achieving the best thermal properties for NextDent. Higher flexibility indicated by prominent skeletal C-C stretching might lead to a lower  $T_g$ , as the polymer chains can move more freely at lower temperatures [52]. For Tera Harz, the findings indicate a different optimal polymerization strategy. The 4 s polymerization time

serves as the control, with no significant differences in Tg observed for polymerization times of 2, 2.4, or 3 s, indicating similar thermal stability across these durations. However, a significant increase in Tg is noted at 4.5 s, indicating that longer polymerization enhances the thermal stability of Tera Harz. These results align with the broader literature, which consistently shows that the degree of polymerization and cross-link density are key determinants of Tg [53]. Higher cross-link densities typically correlate with higher Tg due to reduced molecular mobility within the polymer network [54]. For NextDent, a 7 s polymerization time appears optimal for achieving high thermal stability, while for Tera Harz, a polymerization time of 4.5 s is recommended to enhance Tg and thermal stability. The correlation analysis among E', Tg, and DC reveals important insights into the material properties of polymer-based dental resins. The significant positive correlation between E' and Tg indicates a direct relationship between the mechanical strength and thermal stability of the material. This implies that as the stiffness of the resin increases, so does its resistance to thermal deformation, likely due to a denser cross-linked polymer network [54]. Conversely, the moderate negative correlation between Tg and DC indicates a trade-off between thermal stability and the extent of polymerization. This relationship suggests that achieving higher Tg might involve conditions that lead to a lower degree of monomer conversion. This inverse relationship highlights the challenge of optimizing both properties simultaneously and suggests that adjustments in polymerization protocols might be needed to balance these attributes effectively. The lack of a significant correlation between E' and DC indicates that while both properties are influenced by the polymerization process, they are not directly dependent on each other. This suggests that other factors, such as the nature of the monomers and the specifics of the polymerization process, play a more significant role in determining the storage modulus independently of the degree of conversion. Our findings on the polymerization times and material properties of NextDent Orto Flex and Tera Harz TC 85 have important clinical implications for dental aligners. Tera Harz TC 85's higher degree of conversion (DC) indicates fewer residual monomers, potentially making it healthier for patients. However, its lower glass transition temperature means it could become rubbery in the mouth due to temperature variations. On average, an oral temperature of approximately 34 °C can be measured over a 24 h period [55]. Temperature naturally fluctuates due to factors such as food and beverage intake, ambient temperature changes, mouth breathing, and smoking. For instance, Barclay et al. observed temperatures ranging from 1.62 °C to 65.43 °C during the consumption of hot or cold beverages [56]. NextDent Orto Flex, with its higher storage modulus and Tg, offers greater rigidity and stability at higher temperatures, ideal for applying significant orthodontic forces. However, its lower DC raises concerns about residual monomers and potential health implications. Future studies are needed to further evaluate the long-term health effects and performance of these materials under varying clinical conditions. This study has several limitations, including limited sample size and diversity, which may affect the generalizability of the results. The experiments were conducted under controlled laboratory conditions that do not fully replicate the dynamic environment of the oral cavity, where factors such as saliva, varying pH levels, and mechanical wear could influence material properties. Additionally, the study focused on specific UV exposure durations and immediate material properties post-polymerization, necessitating further research to explore a broader range of exposure times, long-term performance, and potential health implications of residual monomers. Finally, patient comfort and clinical efficacy were not assessed, which are crucial for the practical application of dental aligners.

## 5. Conclusions

Tera Harz TC 85 generally achieves higher DC and more stable polymerization across different UV exposure times than NextDent Orto Flex. Optimal polymerization times significantly impact both the mechanical and thermal properties of these dental resins, with NextDent showing optimal properties at 7 s and Tera Harz benefiting from both very short and extended exposure times. While Tera Harz offers safer polymerization, careful

consideration of its thermal properties is crucial in clinical use due to the risk of it becoming less stable at mouth temperature. In contrast, NextDent Orto Flex, with a higher storage modulus and Tg, provides greater rigidity and stability at elevated temperatures, making it ideal for applying orthodontic forces, though its lower DC raises concerns about residual monomers and associated health risks. These findings underscore the need for tailored curing protocols to maximize the performance of various dental resin formulations.

**Author Contributions:** Conceptualization, L.Š., I.B., T.H. and S.M.; methodology, L.Š., I.B., T.H. and S.M.; software, L.Š., A.J.M. and S.M.; validation, L.Š. and S.M.; formal analysis, L.Š., A.J.M., I.B., T.H. and S.M.; investigation, L.Š., A.J.M., I.B., T.H. and S.M.; resources, I.B., T.H. and S.M.; data curation, L.Š., A.J.M. and S.M.; writing—original draft preparation, L.Š. and S.M.; writing—review and editing, L.Š., A.J.M., I.B., T.H. and S.M.; visualization, L.Š. and S.M.; supervision, S.M.; project administration, L.Š. and S.M.; funding acquisition, L.Š. and S.M. All authors have read and agreed to the published version of the manuscript.

**Funding:** This research received no external funding.

**Institutional Review Board Statement:** The study was conducted in accordance with the Declaration of Helsinki and approved by the Institutional Review Board (or Ethics Committee) of School of Dental Medicine University of Zagreb (05-PA-30-18-5/2023).

**Informed Consent Statement:** Not applicable.

**Data Availability Statement:** The data presented in this study are available on request from the corresponding author due to privacy and ethical restrictions of the School of Dental Medicine University of Zagreb.

**Conflicts of Interest:** The authors declare no conflicts of interest.

## References

1. AlMogbel, A. Clear Aligner Therapy: Up to Date Review Article. *J. Orthod. Sci.* **2023**, *12*, 37. [[CrossRef](#)] [[PubMed](#)]
2. Goracci, C.; Juloski, J.; D'Amico, C.; Balestra, D.; Volpe, A.; Juloski, J.; Vichi, A. Clinically Relevant Properties of 3D Printable Materials for Intraoral Use in Orthodontics: A Critical Review of the Literature. *Materials* **2023**, *16*, 2166. [[CrossRef](#)]
3. Narongdej, P.; Hassanpour, M.; Alterman, N.; Rawlins-Buchanan, F.; Barjasteh, E. Advancements in Clear Aligner Fabrication: A Comprehensive Review of Direct-3D Printing Technologies. *Polymers* **2024**, *16*, 371. [[CrossRef](#)]
4. Ganta, G.K.; Cheruvu, K.; Ravi, R.K.; Reddy, R.P. Clear Aligners, the Aesthetic Solution: A Review. *Int. J. Dent. Mater.* **2021**, *3*, 90–95. [[CrossRef](#)]
5. Staderini, E.; Chiusolo, G.; Guglielmi, F.; Papi, M.; Perini, G.; Tepedino, M.; Gallenzi, P. Effects of Thermoforming on the Mechanical, Optical, Chemical, and Morphological Properties of PET-G: In Vitro Study. *Polymers* **2024**, *16*, 203. [[CrossRef](#)] [[PubMed](#)]
6. Tartaglia, G.; Mapelli, A.; Maspero, C.; Santaniello, T.; Serafin, M.; Farronato, M.; Caprioglio, A. Direct 3D Printing of Clear Orthodontic Aligners: Current State and Future Possibilities. *Materials* **2021**, *14*, 1799. [[CrossRef](#)]
7. Lovestead, T.M.; O'Brien, A.K.; Bowman, C.N. Models of Multivinyl Free Radical Photopolymerization Kinetics. *J. Photochem. Photobiol. A Chem.* **2003**, *159*, 135–143. [[CrossRef](#)]
8. Bichu, Y.M.; Alwafi, A.; Liu, X.; Andrews, J.; Ludwig, B.; Bichu, A.Y.; Zou, B. Advances in Orthodontic Clear Aligner Materials. *Bioact. Mater.* **2022**, *22*, 384–403. [[CrossRef](#)] [[PubMed](#)]
9. Yu, X.; Li, G.; Zheng, Y.; Gao, J.; Fu, Y.; Wang, Q.; Huang, L.; Pan, X.; Ding, J. 'Invisible' Orthodontics by Polymeric 'Clear' Aligners Molded on 3D-Printed Personalized Dental Models. *Regen. Biomater.* **2022**, *9*, rbac007. [[CrossRef](#)]
10. Jindal, P.; Juneja, M.; Siena, F.; Bajaj, D.; Breedon, P. Mechanical and Geometric Properties of Thermoformed and 3D Printed Clear Dental Aligners. *Am. J. Orthod. Dentofac. Orthop.* **2019**, *156*, 694–701. [[CrossRef](#)]
11. Šimunović, L.; Jurela, A.; Sudarević, K.; Bačić, I.; Haramina, T.; Meštrović, S. Influence of Post-Processing on the Degree of Conversion and Mechanical Properties of 3D-Printed Polyurethane Aligners. *Polymers* **2024**, *16*, 17. [[CrossRef](#)] [[PubMed](#)]
12. Mattle, M.; Zinelis, S.; Polychronis, G.; Makou, O.; Panayi, N.; Papageorgiou, S.N.; Eliades, T. Effect of Heat Treatment and Nitrogen Atmosphere during Post-Curing on Mechanical Properties of 3D-Printed Orthodontic Aligners. *Eur. J. Orthod.* **2024**, *46*, cjad074. [[CrossRef](#)] [[PubMed](#)]
13. Aati, S.; Akram, Z.; Shrestha, B.; Patel, J.; Shih, B.; Shearston, K.; Ngo, H.; Fawzy, A. Effect of Post-Curing Light Exposure Time on the Physico-Mechanical Properties and Cytotoxicity of 3D-Printed Denture Base Material. *Dent. Mater.* **2022**, *38*, 57–67. [[CrossRef](#)]
14. Lim, J.H.; Lee, S.Y.; Gu, H.; Jin, G.; Kim, J.E. Evaluating Oxygen Shielding Effect Using Glycerin or Vacuum with Varying Temperature on 3D Printed Photopolymer in Post-Polymerization. *J. Mech. Behav. Biomed. Mater.* **2022**, *130*, 105170. [[CrossRef](#)]
15. Šimunović, L.; Čekalović Agović, S.; Marić, A.J.; Bačić, I.; Klarić, E.; Uribe, F.; Meštrović, S. Color and Chemical Stability of 3D-Printed and Thermoformed Polyurethane-Based Aligners. *Polymers* **2024**, *16*, 1067. [[CrossRef](#)]

16. Przybytek, A.; Gubańska, I.; Kucińska-Lipka, J.; Janik, H. Polyurethanes as a Potential Medical-Grade Filament for Use in Fused Deposition Modeling 3D Printers—A Brief Review. *Fibres Text. East. Eur.* **2018**, *26*, 120–125. [[CrossRef](#)]
17. Cintora-López, P.; Arrieta-Blanco, P.; Martin-Vacas, A.; Paz-Cortés, M.M.; Gil, J.; Aragonese, J.M. In Vitro Analysis of the Influence of the Thermocycling and the Applied Force on Orthodontic Clear Aligners. *Front. Bioeng. Biotechnol.* **2023**, *11*, 1321495. [[CrossRef](#)]
18. Šimunović, L.; Jurela, A.; Sudarević, K.; Bačić, I.; Meštrović, S. Differential Stability of One-layer and Three-layer Orthodontic Aligner Blends under Thermocycling: Implications for Clinical Durability. *Acta Stomatol. Croat.* **2023**, *57*, 286–299. [[CrossRef](#)] [[PubMed](#)]
19. Shaik, A.; Huynh, N.; Youssef, G. Micromechanical Behavior of Ultraviolet-Exposed Polyurea. *Mech. Mater.* **2020**, *140*, 103244. [[CrossRef](#)]
20. Whitten, I.; Youssef, G. The Effect of Ultraviolet Radiation on Ultrasonic Properties of Polyurea. *Polym. Degrad. Stab.* **2016**, *123*, 88–93. [[CrossRef](#)]
21. Dizon, J.; Espera, A.; Chen, Q.; Advíncula, R. Mechanical Characterization of 3D-Printed Polymers. *Addit. Manuf.* **2018**, *20*, 44–67. [[CrossRef](#)]
22. Raza, S.; Nazeer, S.; Abid, A.; Huang, J. Recent research progress in the synthesis, characterization and applications of hyper cross-linked polymer. *J. Polym. Res.* **2023**, *30*, 415. [[CrossRef](#)]
23. Ashfaq, A.; Clochard, M.C.; Coqueret, X.; Dispenza, C.; Driscoll, M.S.; Ulański, P.; Al-Sheikhly, M. Polymerization Reactions and Modifications of Polymers by Ionizing Radiation. *Polymers* **2020**, *12*, 2877. [[CrossRef](#)] [[PubMed](#)]
24. Oliveira, M.S.; da Luz, F.S.; da Costa Garcia Filho, F.; Pereira, A.C.; de Oliveira Aguiar, V.; Lopera, H.A.C.; Monteiro, S.N. Dynamic Mechanical Analysis of Thermally Aged Figue Fabric-Reinforced Epoxy Composites. *Polymers* **2021**, *13*, 4037. [[CrossRef](#)]
25. Dalaie, K.; Fatemi, S.; Ghaffari, S. Dynamic Mechanical and Thermal Properties of Clear Aligners after Thermoforming and Aging. *Prog. Orthod.* **2021**, *22*, 15. [[CrossRef](#)]
26. Youssef, G.; Whitten, I. Dynamic Properties of Ultraviolet-Exposed Polyurea. *Mech. Time-Depend. Mater.* **2017**, *21*, 351–363. [[CrossRef](#)]
27. Xie, R.; Weisen, A.R.; Lee, Y.; Aplan, M.A.; Fenton, A.M.; Masucci, A.E.; Kempe, F.; Sommer, M.; Pester, C.W.; Colby, R.H.; et al. Glass Transition Temperature from the Chemical Structure of Conjugated Polymers. *Nat. Commun.* **2020**, *11*, 893. [[CrossRef](#)]
28. Suteja, T.; Soesanti, A. Mechanical Properties of 3D Printed Polylactic Acid Product for Various Infill Design Parameters: A Review. *J. Phys. Conf. Ser.* **2020**, *1569*, 042010. [[CrossRef](#)]
29. Dewaele, M.; Asmussen, E.; Peutzfeldt, A.; Munksgaard, E.; Benetti, A.; Finné, G.; Leloup, G.; Devaux, J. Influence of Curing Protocol on Selected Properties of Light-Curing Polymers: Degree of Conversion, Volume Contraction, Elastic Modulus, and Glass Transition Temperature. *Dent. Mater.* **2009**, *25*, 1576–1584. [[CrossRef](#)]
30. Tan, J.H.; Chen, C.L.; Wu, J.Y.; He, R.; Liu, Y.W. The effect of UV radiation ageing on the structure, mechanical and gas permeability performances of ethylene-propylene-diene rubber. *J. Polym. Res.* **2021**, *28*, 81. [[CrossRef](#)]
31. Thiessen, M.; Abetz, V. Influence of the Glass Transition Temperature and the Density of Crosslinking Groups on the Reversibility of Diels-Alder Polymer Networks. *Polymers* **2021**, *13*, 1189. [[CrossRef](#)] [[PubMed](#)]
32. Cristea, M.; Ionita, D.; Iftime, M.M. Dynamic Mechanical Analysis Investigations of PLA-Based Renewable Materials: How Are They Useful? *Materials* **2020**, *13*, 5302. [[CrossRef](#)] [[PubMed](#)]
33. Nowick, A.S.; Berry, B.S. *Anelastic Relaxation in Crystalline Solids*; Academic Press: New York, NY, USA, 1972.
34. Ennis, C.P.; Kaiser, R.I. Mechanical Studies on the Electron Induced Degradation of Polymethyl Methacrylate and Kapton. *Phys. Chem. Chem. Phys.* **2010**, *12*, 14902–14915. [[CrossRef](#)] [[PubMed](#)]
35. Wang, Z.; Wu, J.; Shi, X.; Song, F.; Gao, W.; Liu, S. Stereocomplexation of Poly(lactic acid) and Chemical Crosslinking of Ethylene Glycol Dimethacrylate (EGDMA) Double-Crosslinked Temperature/pH Dual Responsive Hydrogels. *Polymers* **2020**, *12*, 2204. [[CrossRef](#)]
36. Fouassier, J.P.; Lalevée, J. *Photoinitiators for Polymer Synthesis: Scope, Reactivity, and Efficiency*; Wiley-VCH Verlag GmbH & Co. KGaA: Weinheim, Germany, 2012. [[CrossRef](#)]
37. Lang, M.; Hirner, S.; Wiesbrock, F.; Fuchs, P. A Review on Modeling Cure Kinetics and Mechanisms of Photopolymerization. *Polymers* **2022**, *14*, 2074. [[CrossRef](#)]
38. Bowman, C.N.; Kloxin, C.J. Toward an Enhanced Understanding and Implementation of Photopolymerization Reactions. *AIChE J.* **2008**, *54*, 2775–2795. [[CrossRef](#)]
39. Balcerak, A.; Kabatc-Borc, J.; Czech, Z.; Bartkowiak, M. Latest Advances in Highly Efficient Dye-Based Photoinitiating Systems for Radical Polymerization. *Polymers* **2023**, *15*, 1148. [[CrossRef](#)]
40. De Beer, M.P.; Van Der Laan, H.L.; Cole, M.A.; Whelan, R.J.; Burns, M.A.; Scott, T.F. Rapid, Continuous Additive Manufacturing by Volumetric Polymerization Inhibition Patterning. *Sci. Adv.* **2019**, *5*, eaau8723. [[CrossRef](#)]
41. Van Der Laan, H.L.; Burns, M.A.; Scott, T.F. Volumetric Photopolymerization Confinement through Dual-Wavelength Photoinitiation and Photoinhibition. *ACS Macro Lett.* **2019**, *8*, 899–904. [[CrossRef](#)]
42. Menard, K.P. *Dynamic Mechanical Analysis: A Practical Introduction*; CRC Press: Boca Raton, FL, USA, 2008; ISBN 978-1-4200-8453-2.
43. Zhang, L.; Li, L.; Chen, Y.; Pi, J.; Liu, R.; Zhu, Y. Recent Advances and Challenges in Long Wavelength Sensitive Cationic Photoinitiating Systems. *Polymers* **2023**, *15*, 2524. [[CrossRef](#)]

44. Lai, Y.; Kuang, X.; Yang, W.; Wang, Y.; Zhu, P.; Li, J.; Dong, X.; Wang, D. Dynamic Bonds Mediate  $\pi$ - $\pi$  Interaction via Phase Locking Effect for Enhanced Heat Resistant Thermoplastic Polyurethane. *Chin. J. Polym. Sci.* **2020**, *39*, 154–163. [[CrossRef](#)]
45. Ceylan, G.; Emik, S.; Yalcinyuva, T.; Sunbuloglu, E.; Bozdog, E.; Unalan, F. The Effects of Cross-Linking Agents on the Mechanical Properties of Poly (Methyl Methacrylate) Resin. *Polymers* **2023**, *15*, 2387. [[CrossRef](#)] [[PubMed](#)]
46. Ali, I.L.; Yunus, N.; Abu-Hassan, M.I. Hardness, Flexural Strength, and Flexural Modulus Comparisons of Three Differently Cured Denture Base Systems. *J. Prosthodont.* **2008**, *17*, 545–549. [[CrossRef](#)] [[PubMed](#)]
47. Tang, Q.; Jiang, J.; Li, J.; Zhao, L.; Xi, Z. Effects of Chemical Composition and Cross-Linking Degree on the Thermo-Mechanical Properties of Bio-Based Thermosetting Resins: A Molecular Dynamics Simulation Study. *Polymers* **2024**, *16*, 1229. [[CrossRef](#)]
48. Gojzewski, H.; Guo, Z.; Grzelachowska, W.; Ridwan, M.; Hempenius, M.; Grijpma, D.; Vancso, G. Layer-by-Layer Printing of Photopolymers in 3D: How Weak is the Interface? *ACS Appl. Mater. Interfaces* **2020**, *12*, 8908–8914. [[CrossRef](#)]
49. Panyukov, S. Theory of Flexible Polymer Networks: Elasticity and Heterogeneities. *Polymers* **2020**, *12*, 767. [[CrossRef](#)]
50. Denisin, A.; Pruitt, B. Tuning the Range of Polyacrylamide Gel Stiffness for Mechanobiology Applications. *ACS Appl. Mater. Interfaces* **2016**, *8*, 21893–21902. [[CrossRef](#)]
51. Qu, T.; Nan, G.; Ouyang, Y.; Bieketuexun, B.; Yan, X.; Qi, Y.; Zhang, Y. Structure-Property Relationship, Glass Transition, and Crystallization Behaviors of Conjugated Polymers. *Polymers* **2023**, *15*, 4268. [[CrossRef](#)]
52. Li, T.; Li, H.; Wang, H.; Lu, W.; Osa, M.; Wang, Y.; Mays, J.; Hong, K. Chain Flexibility and Glass Transition Temperatures of Poly(n-alkyl (meth)acrylate)s: Implications of Tacticity and Chain Dynamics. *Polymer* **2020**, *213*, 123207. [[CrossRef](#)]
53. Zheng, X.; Guo, Y.; Douglas, J.; Xia, W. Understanding the Role of Cross-Link Density in the Segmental Dynamics and Elastic Properties of Cross-Linked Thermosets. *J. Chem. Phys.* **2022**, *157*, 064901. [[CrossRef](#)]
54. Li, S.; Jiaping, W.; Wenjuan, Q.; Cheng, J.; Yunna, L.; Wang, D.; Zhang, F. Green Synthesis and Properties of an Epoxy-Modified Oxidized Starch-Grafted Styrene-Acrylate Emulsion. *Eur. Polym. J.* **2020**, *123*, 109412. [[CrossRef](#)]
55. Choi, J.E.; Lyons, K.M.; Kieser, J.A.; Waddell, N.J. Diurnal Variation of Intraoral pH and Temperature. *BDJ Open* **2017**, *3*, 17015. [[CrossRef](#)] [[PubMed](#)]
56. Barclay, C.; Spence, D.; Laird, W. Intra-Oral Temperatures during Function. *J. Oral Rehabil.* **2005**, *32*, 886–894. [[CrossRef](#)] [[PubMed](#)]

**Disclaimer/Publisher’s Note:** The statements, opinions and data contained in all publications are solely those of the individual author(s) and contributor(s) and not of MDPI and/or the editor(s). MDPI and/or the editor(s) disclaim responsibility for any injury to people or property resulting from any ideas, methods, instructions or products referred to in the content.